Available online at www.sciencedirect.com
ScienceDirect
Electrochimica Acta 53 (2008) 5058–5064
ELECTROCHIMICA Acta
www.elsevier.com/locate/electacta

Electrochemical behavior of Ge and GeX_2 (X = O, S) glasses: Improved reversibility of the reaction of Li with Ge in a sulfide medium

Youngsik Kim [a,1], Haesuk Hwang [b], Katherine Lawler [a], Steve W. Martin [a,*], Jaephil Cho [b,2]

[a] Department of Materials Science and Engineering, Iowa State University, 2220 Hoover Hall, Ames, IA 50011, USA
[b] Department of Applied Chemistry, Kumoh National Institute of Technology, Gumi 730-701, South Korea

Received 15 August 2007; received in revised form 26 November 2007; accepted 3 December 2007
Available online 8 December 2007

Abstract

Sulfide glasses have been considered as new anode materials for lithium-ion batteries because their high ionic conductivity (approximately $\geq 10^{-4}$ S/cm) (more than one order of magnitude higher than oxide glasses (approximately $\leq 10^{-6}$ S/cm)) was expected to accelerate Li^+ ion insertion into and extraction from anode materials during charge and discharge reactions. This intrinsic property can yield the reversible lithium-alloying reaction by minimizing the aggregation of lithium-alloy phases leading to the improvement of cycling behavior. To examine sulfide glasses as new anode materials, GeS_2 glass was chosen for study in this work due to its stability in air-atmospheres. The electrochemical properties of the GeS_2 glass were compared with those of the Ge metal and GeO_2 glass. The initial insertion of lithium into the GeX_2 (X = O, S) glasses leads to the formation of Li_2X (X = O, S) phases associated with the irreversible capacity on the first cycle. The improved reversibility of the reaction of lithium with Ge was observed in the Li_2S medium rather than Li_2O one, which leads to the improvement of cycle performance in the GeS_2 glass anode.

Keywords: Germanium; Sulfide glasses; Anode materials; Cycle life; Lithium-ion batteries

1. Introduction

It is known that electrochemically active metal elements such as Si, Ge, Sn, and Sb provide high lithium atom packing densities through the formation of Li alloys (e.g. $Li_{21}Si_5$ and $Li_{22}Sn_5$) and thereby produce high specific capacity; 4010 mAh/g (9340 mAh/cc) for $Li_{21}Si_5$, 959 mAh/g (7000 mAh/cc) for $Li_{22}Sn_5$ [1]. However, the critical problem with these elements when used as anode materials for lithium-ion batteries is that a large volume change occurs during the alloying/dealloying process of lithiation. This causes fragmentation and crack propagation in these materials which in turn reduces the electrical contact among and between particles and the current collector, ultimately leading to a dramatic capacity loss in the battery after a few cycles.

To overcome this problem, recent research has focused on encapsulating the active materials in a Li^+ conducting matrix so that volume expansion is minimized and the mechanical stress caused by volume changes of the active material can be dissipated inside the matrix. This idea has been shown to work well for tin composite oxide (TCO) glasses such as $SnO + B_2O_3 + P_2O_5 + Al_2O_3$ [2,3] and $SnO + B_2O_3 + P_2O_5$ [4,5]. The gravimetric capacities of these glasses have been found to be more than twice that of commonly used graphite anode (LiC_6) materials [2–5]. In addition, TCO glasses have been found to provide reasonable cycleability in battery performance [4,5]. The reaction mechanism of lithium insertion into TCO glasses is thought to be similar to that for SnO crystals where initially the Li reacts with SnO to form Li_2O and Sn and the newly isolated Sn embedded in the matrix reacts with subsequent Li uptake to form nano-sized Li-Sn alloys (ultimately $Li_{4.4}Sn$) [4–6]. In this process, the nano-sized Li–Sn alloy particles (related to reversibility) that form in TCO glasses were found to be maintained, while the Li–Sn particles formed in the crystalline SnO continued to grow with continued cycling. The maintenance of the small sized Li–Sn domains is thought to be responsible for the good cycleability of TCO glass anodes. The remaining components such as

* Corresponding author. Tel.: +1 515 294 0745; fax: +1 515 294 5444.
E-mail address: swmartin@iastate.edu (S.W. Martin).
[1] Present address: Texas Materials Institute, The University of Texas at Austin, Austin, Texas 78712, USA.
[2] Present address: Department of Applied Chemistry, Hanyang University, Ansan 426-791, South Korea.

0013-4686/$ – see front matter © 2007 Elsevier Ltd. All rights reserved.
doi:10.1016/j.electacta.2007.12.015

Li–B–P–O (for $SnO + B_2O_3 + P_2O_5$ glass) and Li–B–P–Al–O for ($SnO + B_2O_3 + P_2O_5 + Al_2O_3$ glass) [7–9], which create the amorphous matrix, were reported to prevent the aggregation of the Sn clusters during alloying/dealloying of lithium process. In addition to the remaining components, the amount of oxygen in the matrix was also considered an important factor in enhancing the cyclability of these glassy electrodes [7,8]. Many oxygen atoms intimate contact with Li–Sn domains quickly respond to the isolated Sn particles (after delithiation) through the reverse reaction of Sn to from Sn–O bonds before isolated tin atoms begin to cluster. For these reasons, the TCO glasses show better cycle-life performance compared to the SnO_2 anode material. However, there are still problems that should be solved before using TCO glasses in commercial applications. These include the large irreversible capacity loss in the first charge cycle and the gradual decrease in the cyclability compared to graphite anodes. On the other hand, extensive research has been conducted on amorphous M–A–C systems (M = Sn, Si, Sb, Ge; A = transition metals) [10–12]. While these materials generally have a significant first cycle irreversible capacity, good cycle performance with a high specific capacity has been found in disordered structures in the Sn–Co–C system. These anode materials have recently been commercialized by Sony [13].

In this research effort, sulfide glasses, which are based on the chemistry of sulfur rather than oxygen, are being considered as a new class of anode materials by providing a higher Li^+ ionic conducting medium that will potentially better dissipate the mechanical stresses induced by the large volume changes of lithium alloys through the lower mechanical modulus of the sulfide glasses compared to the oxide glasses.

1.1. High Li^+ ionic conducting sulfide glasses as anode materials

Lithium-ion conductive glasses can be generally divided into two types, oxide glasses and chalcogenide glasses. These glasses are formed by a network glass former such as SiO_2, B_2O_3, or P_2O_5 and a network modifier, Li_2O, to form oxide glasses such as $Li_2O + SiO_2$ [14,15], $Li_2O + B_2O_3$ [15,16], and $Li_2O + P_2O_5$ [17,18] and by network former such as SiS_2, GeS_2, P_2S_5, or B_2S_3 and a network modifier, Li_2S, to form sulfide glasses such as $Li_2S + P_2S_5$ [19], $Li_2S + GeS_2$ [18,20], $Li_2S + SiS_2$ [21], and $Li_2S + B_2S_3$ [22]. As predicted by the Anderson–Stuart model [23] and the weak electrolyte theory [24] the substitution of sulfur for oxygen greatly reduces the bond energy between the lithium cation and sulfur anion and as a result of the greater polarizability of the sulfur the activation energy is thus reduced as shown in Fig. 1a. Therefore, sulfide glasses exhibit much higher ionic conductivities than their oxide counterparts as shown in Fig. 1b [25]. With a maximum Li_2X (X = O, S) content, the conductivity of sulfide glass ($\sigma_{25\,^\circ C} \sim 10^{-4}$ $(\Omega\,cm)^{-1}$) can be two orders of magnitude higher than that of oxide glasses ($\sigma_{25\,^\circ C} \sim 10^{-6}$ $(\Omega\,cm)^{-1}$).

Hence, based on the knowledge that a lithium oxide matrix in the TCO glasses has poor ionic conductivity, the hypothesis has been explored in which sulfide glasses would be able to provide

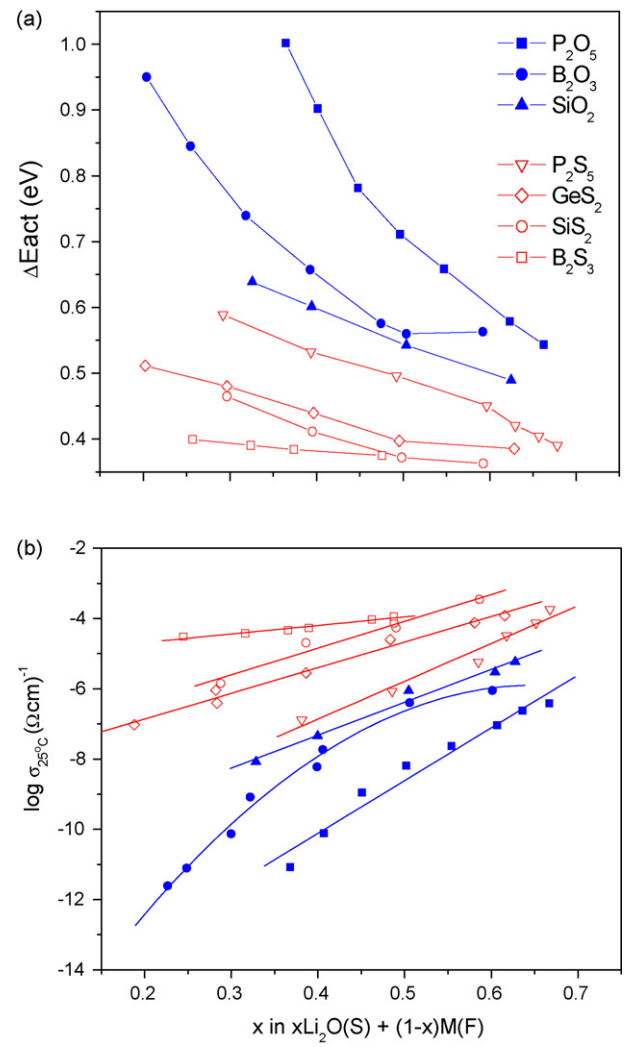

Fig. 1. (a) Activation energy and (b) conductivity variations with the composition for $xLi_2O + (1-x)M$ ($M = SiO_2$, B_2O_3, and P_2O_5) and $xLi_2S + (1-x)F$ ($F = B_2S_3$, SiS_2, GeS_2, and P_2S_5) glasses [25].

a matrix with higher Li^+ ionic conductivity and thereby reduce the internal resistance, resulting in an increased energy density of the anode. In addition, since sulfur is available as a solid-state element (unlike the gas state of oxygen), more flexible compositions of sulfide glasses can be prepared by controlling the amount of sulfur. If the sulfur does play an important role in enhancing cycleability as oxygen does in TCO glasses, sulfide glasses may also have tremendous advantages over oxide glasses because the sulfur content in these glasses can be optimized to improve the cycleability and capacity of anodes. For these reasons, sulfide glasses have been investigated as good candidates for new anode materials in this research group.

Among many possible sulfide glasses, GeS_2 glass was chosen as an electrode material for this study due to its relative chemical stability in air compared to other sulfide glasses which are extremely unstable in air. For this reason, GeS_2 glass would be easy to handle in the lab, especially when preparing the anode plates. GeO_2 glass was also prepared and its electrochemical properties were compared with those of GeS_2 glass to examine

the improved electrochemical characteristics. Since no distinctive peaks were observed in the XRD patterns of the glassy GeO_2 and GeS_2, the lithium reaction mechanism with Ge metal was first studied by XRD measurements and this information was used to interpret the lithium insertion and extraction reactions with the glassy GeO_2 and GeS_2.

2. Experimental methods

2.1. Preparation of the glasses

Vitreous GeS_2 was prepared by mixing and reacting stoichiometric amounts of germanium (Cerac, 99.999%) and sulfur (Cerac, 99.999%) in an evacuated silica tube. The silica tube was rotated at an angle of ∼10° in a tube furnace and heated at 1 °C/min to 900 °C, held for 8 h and then quenched in air. Vitreous GeO_2 was prepared by melting crystalline GeO_2 (Cerac, 99.999%) powders for 1 h at 1400 °C in a platinum crucible and then air quenching to room temperature.

2.2. Fabrication of the button-type electrochemical cells

The electrodes were fabricated from a 80:10:10 (mass %) mixture of active material, binder, and conductive material. Polyvinylidene difluoride (PVDF, Aldrich) was used as the binder and Super-P carbon black (MMM Carbon) was used as the current conductor. The PVDF was dissolved in *N*-methylpyrrolidinone (NMP, Kanto) and then the active material and conductor mixture were added to the homogeneous solution of PVDF and NMP. After further homogenization, the slurry was coated on a thin copper foil (20 μm thick) and dried overnight at 120 °C. The electrode was pressed with a pressure of 600–800 kg/cm^2 and punched into 15 mm diameter disks.

The electrochemical cells were prepared using standard 2016 coin cell hardware with lithium metal foil used as both the counter and reference electrodes. Cells were assembled in an Argon atmosphere glove box. A mixture of ethylene carbonate/diethylene carbonate (EC/DEC) with 1 M $LiPF_6$ salt was used as the electrolyte. The cells were aged for 5 h before the first charge to ensure full absorption of the electrolyte into the electrodes. The cell was then cycled at the rate of 0.1 C (= 134 mA/g) between 0 and 1.5 V on WBCS 3000 battery tester (WonA Tech).

2.3. 2.3. Powder X-ray diffraction

The powder XRD data were collected at 298 K using a Scintag diffractometer with Cu Kα radiation (λ = 1.5406 Å). It was operated at 40 kV and 30 mA in the 2θ range of 10°–70° in the continuous scan mode with step size 0.02° and scan rate 1.0 (°/min). For the *ex-situ* XRD measurements, the cells charged or discharged to certain voltages were disassembled in a glove box and the electrodes were rinsed thoroughly with a DMC solution to remove the $LiPF_6$ salts.

3. Results and discussion

3.1. Electrochemical properties of Ge metal

Fig. 2a shows the voltage profiles of the Li/Ge metal cell over 30 cycles between 0 and 1.5 V at a rate of 0.1 C (=134 mA/g). When the cell of Li/Ge metal is first discharged (Li^+ insertion) to 0 V, a large discharge capacity, 1420 mAh/g, is observed, which corresponds to 3.8 moles of Li^+ ion per mole of Ge metal. The subsequent Li^+ extractions (up to 1.5 V charge) yield the charge capacity of 496 mAh/g, which corresponds to 1.3 moles of Li^+ per mole of Ge metal.

Ex-situ XRD measurements of the Li/Ge cell were performed to investigate the Li^+ insertion/extraction mechanism with Ge metal and they are shown in Fig. 2b. When the cell is first discharged to 0 V, the diffraction peaks of Ge metal, 27.3°, 45.3°, and 53.8°, observed in the pristine plate dramatically decrease,

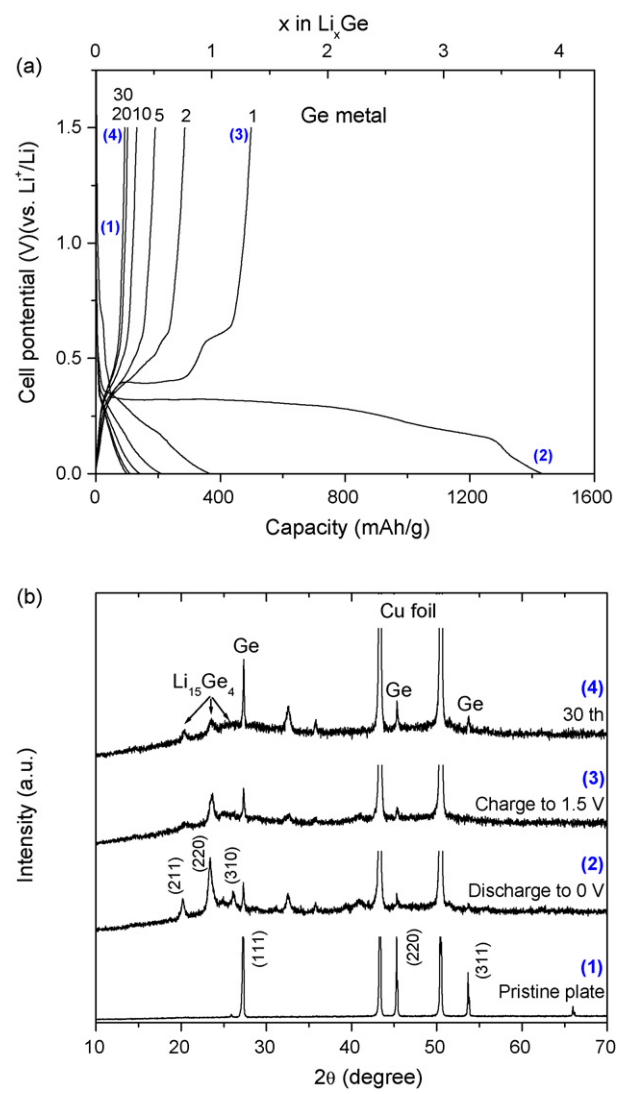

Fig. 2. (a) Voltage profiles of the Ge metal between 1.5 and 0 V at a rate of 0.1 C. (b) The powder X-ray diffraction patterns of Ge electrodes, before discharging at point (1), after fully discharging to 0 V at point (2), after fully charged to 1.5 V at point (3), and after 30 cycles (fully charged to 1.5 V) at point (4).

while the peak observed at 20.2°, 23.4°, and 26.4° assigned for $Li_{15}Ge_4$ phase becomes dominant. Similar to the electrode behavior of Sn metal [26], the first discharge capacity is expected to be the formation of intermediate Li–Ge compositions in the Li–Ge alloy phases such as LiGe [JCPDS No. 77-2492], $Li_{11}Ge_6$ [JCPDS No. 29-0803], Li_9Ge_4 [JCPDS No. 73-2487], Li_7Ge_2 [JCPDS No. 29-0636], $Li_{15}Ge_4$ [JCPDS No. 89-2584], and $Li_{22}Ge_5$ [JCPDS No. 17-0402]. Although $Li_{22}Ge_5$ is the theoretical limit phase in the Li–Ge alloys, the ultimately reacted phase could be $Li_{15}Ge_4$ after discharging to 0 V. The calculated discharge capacity (1384 mAh/g) of $Li_{15}Ge_4$ corresponds with 3.75 moles of Li^+ ions per mole of Ge metal and is comparable to that observed experimentally (3.8 moles of Li^+ ions). The other small peaks observed at 32.6° and 35.8° are not matched with any other known Li–Ge phases. Diffraction peaks at those positions are also observed at the end of the first discharge of the GeO_2 and GeS_2 glass electrodes, but they are not identified at this point.

When the cell is charged (Li^+ extraction) to 1.5 V followed by the first discharge, the peaks assigned to the $Li_{15}Ge_4$ phase still remain as the major feature, which suggests that a large number of Li ions were not reversibly extracted from the $Li_{15}Ge_4$ domains. This may be the cause of the large irreversible capacity after the first discharge. On further cycling, the intensity of the Ge peaks increase as shown in Fig. 2b-(4) and this can be related to the aggregation of Ge grains. In addition to the aggregation of Ge grains, large volume changes, which generally appear when the metallic host is transformed to lithium-alloy phases [26], lead to the formation of cracks in the electrode plate, which eventually yields to the loss of ionic and electronic interparticle contact. This is believed to be the major cause of the poor reversibility observed in the Li/Ge metal cell.

3.2. Electrochemical properties of GeO_2 glass

Compared to the Ge metal electrode, the GeO_2 electrode would be expected to yield different behaviors due to its oxygen content. According to the electrode behavior of SnO_2 [4,6], the initial first discharge capacity of the Li/SnO_2 cell was attributed to the formation of Li_2O and Sn, followed by the formation of Li–Sn phases. A similar mechanism can be observed in GeO_2 cell as well. Fig. 3 shows the voltage profiles of the Li/GeO_2 cell and *ex-situ* XRD measurements. The large capacity, 2000 mAh/g, compared with 1400 mAh/g of Ge metal, is observed on the first discharge curve of the GeO_2 electrode. This corresponds to the larger number of Li^+ ions consumed to form Li_2O phase and Ge metal, followed by the formation of Li–Ge alloys. If the ultimately formed Li–Ge alloy phase is assumed to be $Li_{15}Ge_4$ ($Li_{3.75}Ge$) as observed in the above Li/Ge metal reaction, the following reaction can be expected; $7.75Li + GeO_2 \rightarrow 2Li_2O + Li_{3.75}Ge$. Based on this reaction, the calculated first discharge capacity is 1986 mAh/g and compares well to that of 2000 mAh/g for the observed first discharge capacity.

Therefore, it is expected that the increase in lithium insertion gradually destroys the GeO_2 lattice and leads to the formation of Li_2O and Ge domains. As the Li_2O acts as a lithium cation

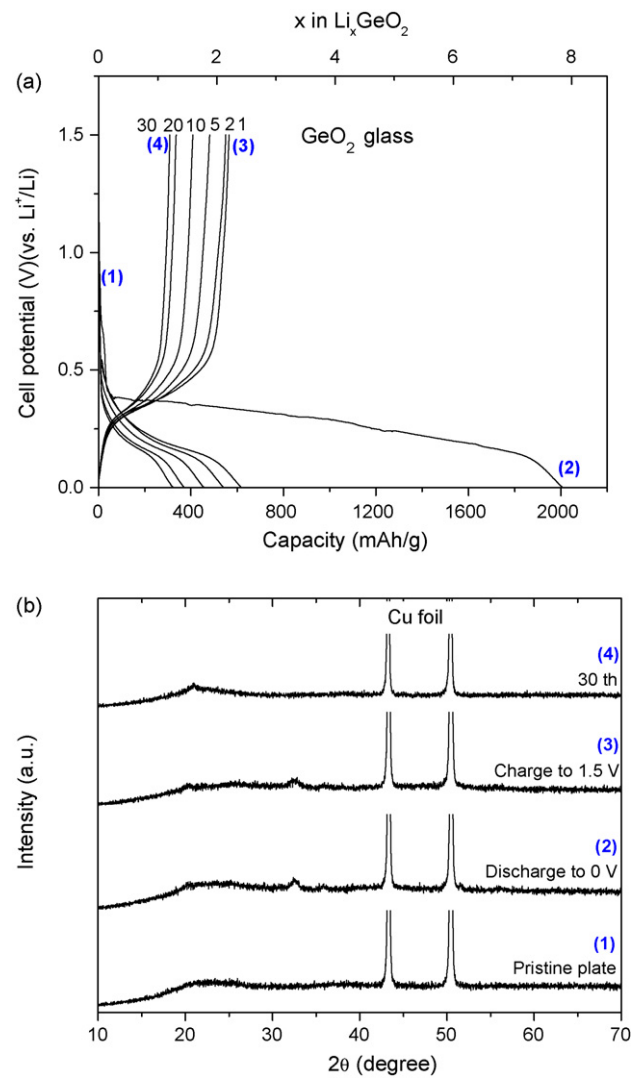

Fig. 3. (a) Voltage profiles of the glassy GeO_2 between 1.5 and 0 V at a rate of 0.1 C. (b) The powder X-ray diffraction patterns of the glassy GeO_2 electrodes, before discharging at point (1), after fully discharging to 0 V at point (2), after fully charged to 1.5 V at point (3), and after 30 cycles (fully charged to 1.5 V) at point (4).

conducting matrix to allow further alloying and dealloying of the active atoms [4,6], the Ge atoms can react with Li^+ ions to form Li–Ge alloy phases during the discharging process. However, any distinctive peaks related to Li_2O and Li–Ge alloys are not observed in the XRD at the end of the first discharge (Fig. 3b-(2)). This is very similar to the results observed in the tin-based oxide glasses [4–6], in which the Li_2O phase formed in these types of materials was suggested to be an amorphous phase and Li–Sn alloy domains were too small to be detected by XRD [4–6]. When the cell is then charged to 1.5 V, those XRD patterns remain and no other diffraction peaks appear even after 30 cycles, indicating no significant phase transition occurs during cycling. The cycle-life of GeO_2 is improved compared to Ge metal as shown in Fig. 5. This can be related to the formation of the Li_2O phase as the Li_2O matrix was known to improve the reversibility of the electrode by reducing the large volume

changes associated with alloying and de-alloying in reversible charge and discharge reactions [4–6].

3.3. Electrochemical properties of GeS_2 glass

The voltage profiles of GeS_2 glass were performed for 30 cycles between 0 and 1.5 V at a rate of 0.1 C (=134 mA/g) and are presented in Fig. 4. The observed first charge and discharge capacities are 1417 and 446 mAh/g, respectively. The large irreversibility capacity for the first cycle would be caused by the formation of Li_2S similar to the case of the GeO_2 glass. Compared to the first discharge curve of the GeO_2 glass, however a more continuous curve slope is observed in that of the GeS_2 glass. Since the voltage curve is related to the reaction steps; for example to the formation of the various lithium–tin alloy phases during Li^+ intercalation and de-intercalation to produce the smooth charge and discharge curves without the characteristic steps [27], more numerous Li–Ge alloy phases are thought to be formed during Li^+ intercalation into GeS_2 glass compared to that of GeO_2 glass. Although the large irreversibility capacity is still observed in the first cycle of the GeS_2 glass, much improved cyclability, 93% of capacity retention after 30 cycles, is observed in the following cycles compared to that of the GeO_2 glass. This is superior not only to that of GeO_2 glasses (Fig. 5), but also to that previously reported for the TCO glasses [4–6,28,29]. Similar to the case of GeO_2 glass, there are no distinctive XRD patterns found during the discharging and charging process of GeS_2 glass. This measurement is limited in its ability to obtain more detailed reaction mechanisms between lithium and these glassy samples because no obvious diffraction peaks appear in both samples.

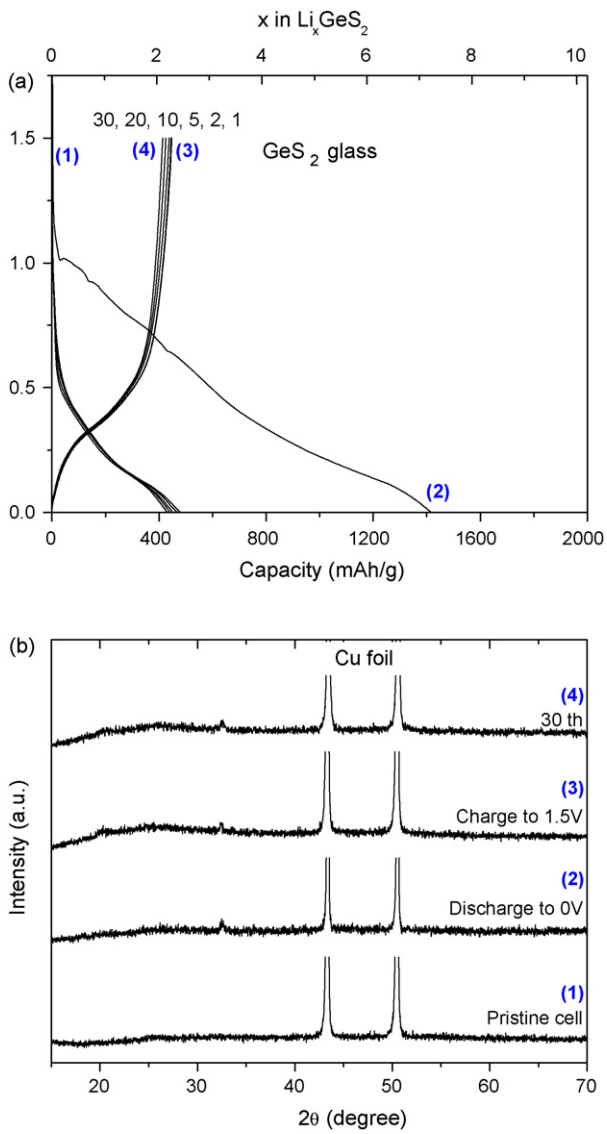

Fig. 4. (a) Voltage profiles of the glassy GeS_2 between 1.5 and 0 V at a rate of 0.1 C. (b) The powder X-ray diffraction patterns of the glassy GeS_2 electrodes, before discharging at point (1), after fully discharging to 0 V at point (2), after fully charged to 1.5 V at point (3), and after 30 cycles (fully charged to 1.5 V) at point (4).

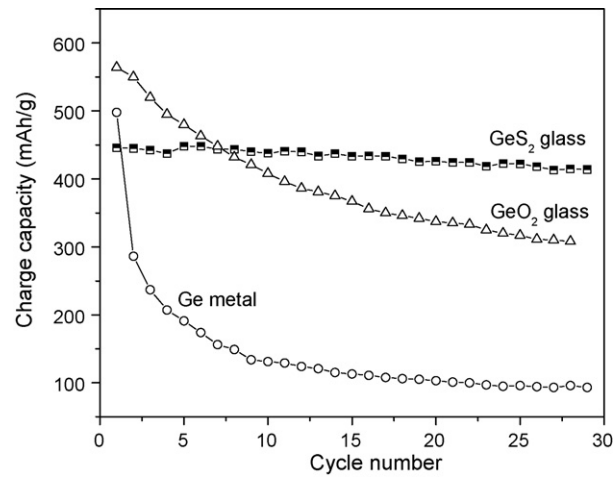

Fig. 5. Cycle-life performance of Ge metal, GeO_2 glass, and GeS_2 glass, respectively. They are operated between 1.5 and 0 V at the rate of 0.1 C.

To further investigate the lithium insertion/extraction mechanism of GeS_2 glass, a differential capacity plot was constructed from the voltage profiles and compared with that of GeO_2 glass. This property has been known to be a sensitive detector of phase transformation in the electrode material from cycle to cycle. Fig. 6 shows the differential capacity plots of the 1st, 2nd, 10th, and 30th cycle curves for GeS_2 and GeO_2 glasses, respectively. In the first curves for both samples, the sharp irreversible cathodic peaks appear between 0.2 and 0.5 V for the GeO_2 glass, and between 0.2 and 1.3 V for the GeS_2 glass. However, the subsequent anodic and cathodic peaks are reversible and appear at ~0.35 and ~0.15 V, respectively, for both glasses. As discussed above, the initial insertion of lithium into the GeX_2 (X = O, S) glasses leads to the formation of Li_2X (X = O, S) and Li–Ge phases, which are irreversible and reversible, respectively, with the reaction of lithium on further cycling. Hence, the reversible anode peaks at ~0.35 V and cathode peaks at ~0.15 V in the differential capacity plots for both glasses are related to the lithium insertion and extraction reactions, respectively, associated with alloying and de-alloying of Li–Ge phases. On the other hand, the irreversible sharp cathodic peaks observed on the first cycle curves are associated with the decomposition of the GeX_2

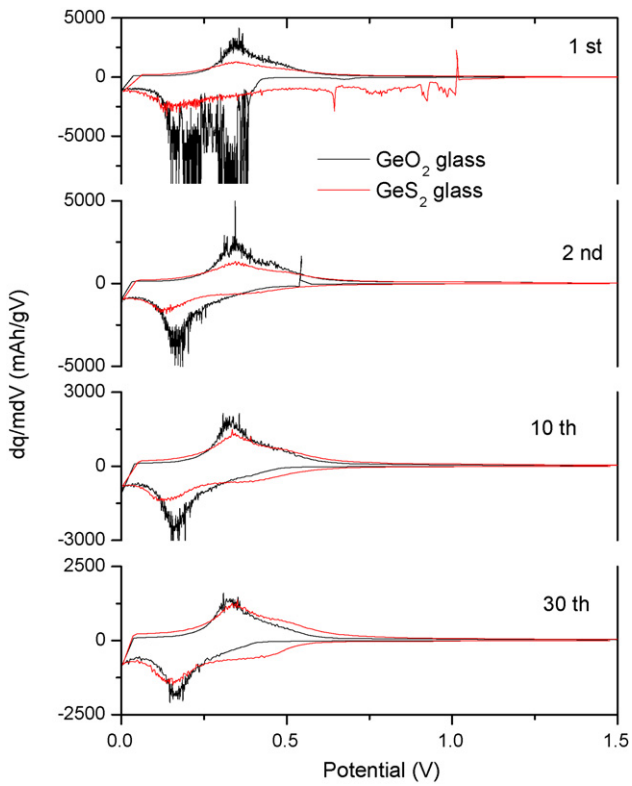

Fig. 6. Differential capacity plots of Li/GeO_2 glass and Li/GeS_2 glass cells for the 1st, 2nd, 10th, and 30th cycled between 1.5 and 0.0 V.

(X = O, S) glasses and the formation of Li_2X (X = O, S) phases. Similar results are also observed in the TCO glasses [28,29].

After the first cycle, the differential capacity curves of GeS_2 glass are observed to be smoother than those of the GeO_2 glass. As alloy-type materials with smooth differential capacity curves generally cycle better than those with sharp peaks in these curves [5], the constancy of the plots of GeS_2 glass is indicative of the good reversibility of the electrode material in repetitive charge and discharge operations, which correspond well with the cycle-life shown in Fig. 5. In addition, the single and smooth cathodic and anodic peaks corresponding to the alloying and de-alloying processes are indicative of the improved homogeneity of the Ge environments. In contrast, the reversible cathodic and anodic peaks observed in the differential capacity plots of GeO_2 glass are sharp with many spikes, which can be associated with the aggregation of Li–Ge alloys.

Since the reversibility of these types of materials lies in controlling and eliminating the aggregation of lithium-alloy grains into large clusters [4–8], there should be something in the GeS_2 glass that helps to limit the aggregation of Li–Ge alloys and Ge atoms. As discussed above, the Li_2O and Li_2S amorphous phases, which are formed by the decomposition of GeO_2 and GeS_2, respectively, could act as a matrix by surrounding and binding the Li–Ge alloy domains together, which eventually decrease the volume changes between the Ge and Li–Ge domains. Li^+ ions will be more mobile in the sulfide matrix compared to the oxide matrix. In addition, the electron mobility in the matrix will be also greater because the sulfur atoms provide a greater electron population in the matrix. For these reasons, it is believed that the higher Li^+ and electron conductivities of the sulfide matrix can accelerate Li^+ ion transportation between Ge and Li–Ge domains through the matrix, and can possibly help retard the aggregation of those Li–Ge alloy domains.

4. Conclusions

Sulfide glasses have been considered as promising anode materials for lithium-ion batteries due to their high ionic conductivity. GeS_2 glass was first investigated in this work due to its chemical stability in air atmospheres. The electrochemical properties of the GeS_2 glass were compared with those of the GeO_2 glass. A large irreversible capacity loss was observed in the first cycle for both of the GeO_2 and GeS_2 glasses. From XRD and differential capacity plots, this irreversible capacity loss was expected to be the result of the decomposition of the starting materials and formation of Li_2O for the GeO_2 phase and Li_2S for the GeS_2 phase. Li–Ge alloy phases were also formed in both cases and the alloying and de-alloying reactions for these phases were responsible for the cycleability of the electrodes in the following cycles. Compared to the GeO_2 phases, better reversibility was observed for the GeS_2 glass. This is believed to be due to the fact that the Li_2S matrix provides for fast Li^+ ionic and electronic conductivity so that the aggregation of Li–Ge domains would be retarded by the fast Li^+ transportation between Ge and Li–Ge alloys.

Controlling the aggregation of active atoms into large clusters was known to be the key to improve the cycling behavior in these of type materials, and strategies developed with this work can provide a new direction for better anode materials. The large irreversible capacity in the first cycle may create difficulties in the practical application of these materials in lithium-ion cells. However, there are many other possible sulfide glass systems that can be investigated to find a better medium for ionic and electronic conduction and also minimize the irreversible capacity loss. In addition, there remains much to do to understand the physics, chemistry, and materials science of the reaction of lithium with sulfide glasses. Our future work will focus on binary or even ternary sulfide glasses containing at least one spectator atom that does not react with lithium ions because the spectator atoms are known to disperse active particles in the matrix and retard their aggregation during cycling.

References

[1] G.A. Nazri, G. Pistoia, Lithium Batteries: Science and Technology, Kluwer Academic Publishers, Boston, 2004, p. 116.
[2] Y. Idota, A. Matsufuji, Y. Maekawa, T. Miyasaki, Science 276 (1997) 13975.
[3] Y. Idota, M. Nishima, Y. Miyaki, T. Kubota, T. Miyasaki, Can. Pat. Appl. 2,134,053 (1994).
[4] I.A. Courtney, J.R. Dahn, J. Electrochem. Soc. 144 (1997) 2943.
[5] I.A. Courtney, W.R. McKinnon, J.R. Dahn, J. Electrochem. Soc. 146 (1999) 59.
[6] I.A. Courtney, J.R. Dahn, J. Electrochem. Soc. 144 (1997) 2045.
[7] G.R. Goward, F. Leroux, W.P. Power, G. Ouvrard, W. Dmowski, T. Egami, L.F. Nazar, Electrochem. Solid-State Lett. 2 (1999) 367.
[8] G.R. Goward, L.F. Nazar, W.P. Power, J. Mater. Chem. 10 (2000) 1241.

[9] L.F. Nazar, G. Goward, F. Leroux, M. Duncan, H. Huang, T. Kerr, J. Gaubicher, Int. J. Inorg. Mater. 3 (2001) 191.
[10] S. Kawakami, M. Asao, Eur. Pat. Appl. EP103,956,8A1 (2000).
[11] J.R. Dahn, R.E. Mar, A. Abouzeid, J. Electrochem. Soc. 153 (2) (2000) A361.
[12] M.N. Obrovac, L. Christensen, D.B. Le, J.R. Dahn, J. Electrochem. Soc. 154 (9) (2007) A849.
[13] http://www.sony.net/SonyInfo/News/Press/200502/05-006E/.
[14] M. Yoshiyagawa, M. Tomozawa, J. Phys. Colloque. C 9 (1982) 411.
[15] M. Tatsumisago, K. Yoneda, N. Machida, T. Minami, J. Non-Cryst. Solids 95–96 (1987) 857.
[16] S. Smedley, C.A. Angell, Mater. Res. Bull. 15 (1980) 421.
[17] S.W. Martin, C.A. Angell, J. Non Cryst. Solids 83 (1986) 185.
[18] A. Pradel, T. Pagnier, M. Ribes, Solid State Ionics 17 (1985) 147.
[19] R. Mercier, J.P. Malugani, B. Fahys, A. Saida, Solid State Ionics 5 (1981) 663.
[20] M. Ribes, B. Barrau, J.L. Souquet, J. Non-Cryst. Solids 38–39 (1980) 271.
[21] A. Pradel, M. Ribes, Solid State Ionics 18–19 (1986) 351.
[22] A. Leavasseur, R. Olazcuaga, M. Kbala, M. Zahi, P. Hagenmuller, C. R. Acad. Sci. Paris 293 (1981) 563.
[23] O. Anderson, D. Stuart, J. Am. Ceram. Soc. 37 (1954) 573.
[24] D. Ravaine, J.L. Souquet, Phys. Chem. Glasses 18 (1977) 27.
[25] A. Pradel, M. Ribes, Mater. Chem. Phys. 23 (1989) 121.
[26] M. Winter, J.O. Besenhard, Electrochim. Acta 45 (1999) 31.
[27] R.A. Higgins, J.O. Besenhard, Handbook of Battery Materials, Wiley-VCH, Weinheim, 1998, p. 359.
[28] Y.W. Xiao, J.Y. Lee, A.S. Yu, Z.L. Liu, J. Electrochem. Soc. 146 (1999) 3623.
[29] J.Y. Lee, Y. Xiao, Z. Liu, Solid State Ionics 133 (2000) 25.